

Supporting Information for

Dimethyl yellow-based colorimetric chemosensors for “naked eye” detection of Cr³⁺ in aqueous media *via* test papers

De-Hui Wang,^{‡,a*} Yuan Zhang,^{‡,b} Ran Sun^a and De-Zhi Zhao^{a*}

^a College of chemistry, chemical engineering and environmental engineering,
Liaoning Shihua University, Fushun, 113001, China

^b Liaoning Institute for Food Control, Shenyang, 110015, China.

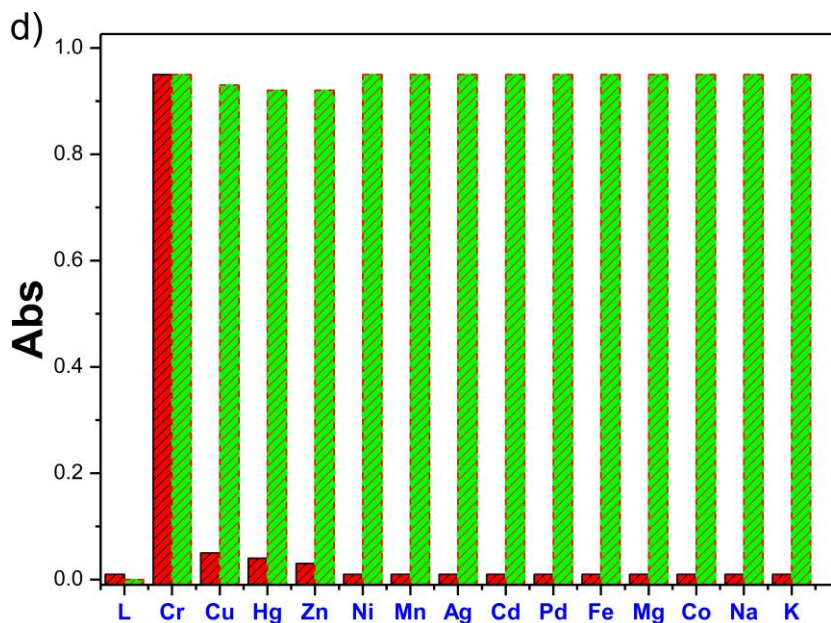
E-mail: dhuiwang@aliyun.com

[‡] D. Wang and Y. Zhang contributed equally to this work.

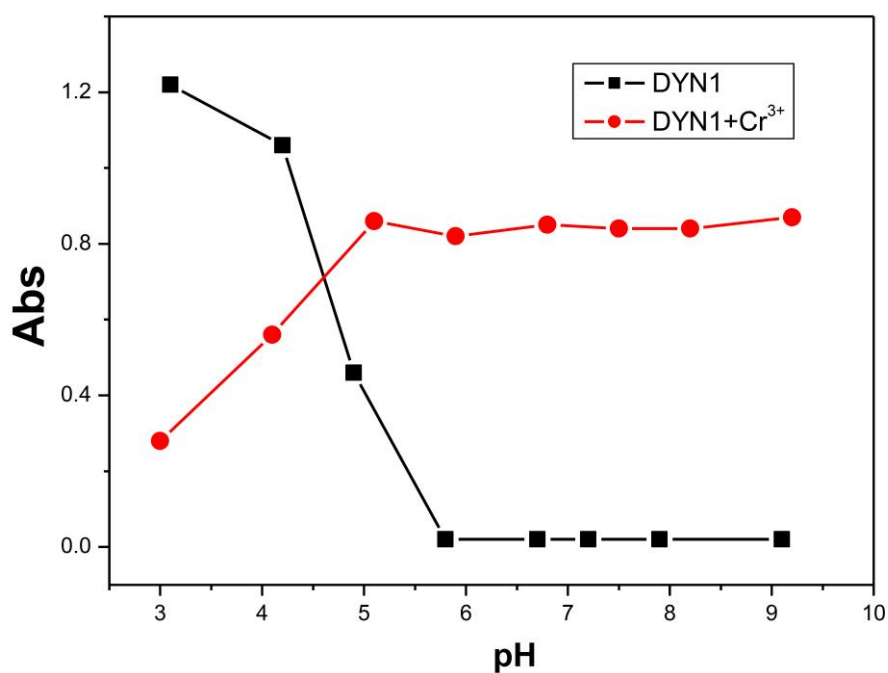
Table of Contents

1. **Figure S1** Selectivity and competition of **DYN1** for Cr³⁺
2. **Figure S2** The pH-dependent of **DYN1** and **DYN1+Cr³⁺**
3. **Figure S3** Calculations for detection limit of **DYN1** with Cr³⁺
4. **Figure S4** Selectivity and competition of **DYN3** for Cr³⁺
5. **Figure S5** The pH-dependent of **DYN3** and **DYN3+Cr³⁺**
6. **Figure S6** Calculations for detection limit of **DYN3** with Cr³⁺
7. **Figure S7** Selectivity and competition of **DYN2** for Cr³⁺
8. **Figure S8** The pH-dependent of **DYN2** and **DYN2+Cr³⁺**
9. **Figure S9** Calculations for detection limit of **DYN2** with Cr³⁺
10. **Figure S10** ¹H-NMR spectra of **DYN1**
11. **Figure S11** ¹H-NMR spectra of **DYN3**
12. **Figure S12** ¹H-NMR spectra of **DYN2**
13. **Figure S13** ¹H-NMR spectra of **DYN4**
14. **Figure S14** ¹H-NMR spectra of **1**
15. **Figure S15** ¹H-NMR spectra of **2**
16. **Figure S16** ¹H-NMR spectra of **3**
17. **Figure S17** Contour plots of the HOMO and LUMO for **DYN1-4**
18. **Figure S18** ESI-TOF spectra of **DYN1+Cr³⁺**
19. **Figure S19** ICP-AES spectra of sewage sample

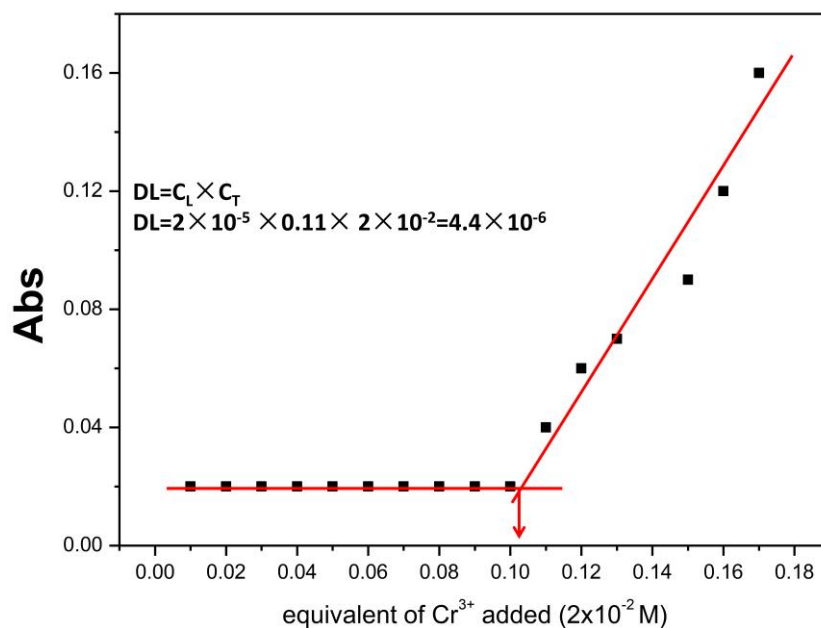
1. **Figure S1** UV-Vis spectra of **DYN1** (2×10^{-5} M) in $\text{CH}_3\text{CN}:\text{H}_2\text{O}$ (1:1, v/v, containing 0.01 M HEPES, pH=7.21) upon titration with 3.0 equiv. of perchlorate salts of metals. The red bars represent the absorbance of **DYN1** in the presence of 2 equiv. of cations of interest, respectively. The green bars represent the absorbance that occur upon the subsequent addition of 2 equiv. of Cr^{3+} to the above mentioned solutions, respectively. The absorbance measurements were recorded at 516 nm.



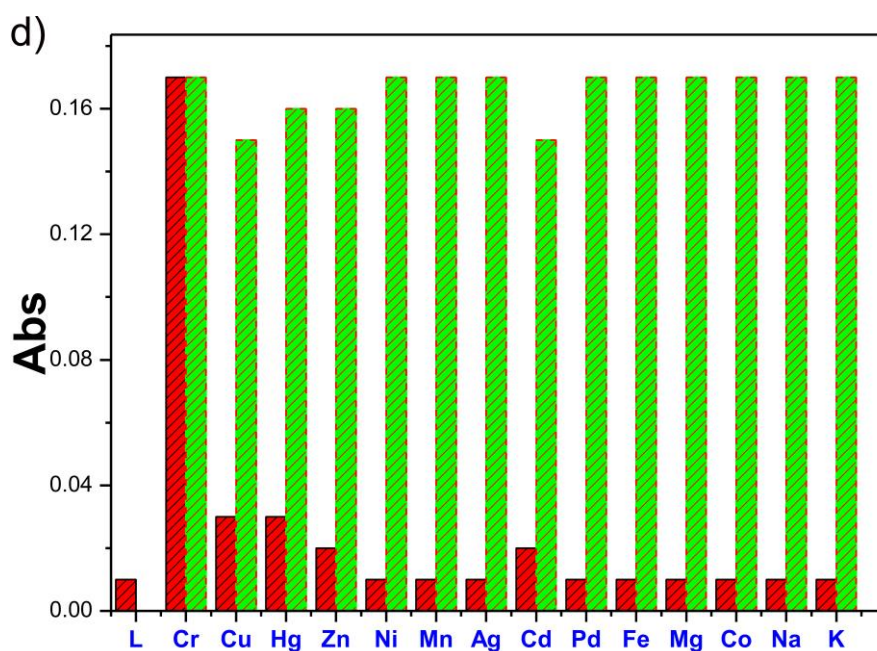
2. **Figure S2** The pH-dependent absorbance response of **DYN1** (20 μM) and **DYN1**+ Cr^{3+} in $\text{CH}_3\text{CN}/\text{H}_2\text{O}$ (1:1, v/v). The absorbance measurements were recorded at 516 nm.



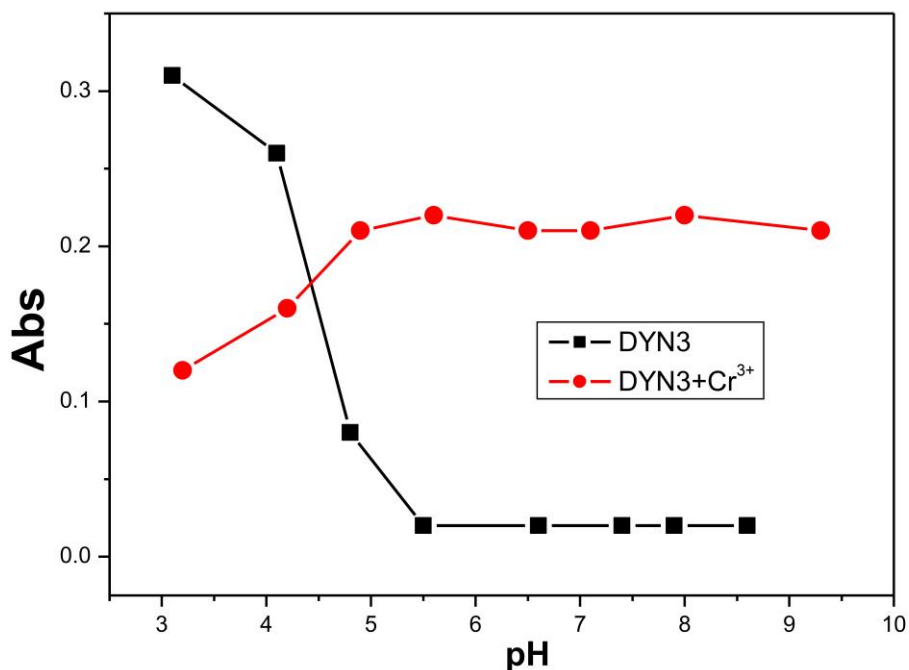
3. **Figure S3** Calculations for detection limit of **DYN1** with Cr^{3+} . The absorbance measurements were recorded at 516 nm.



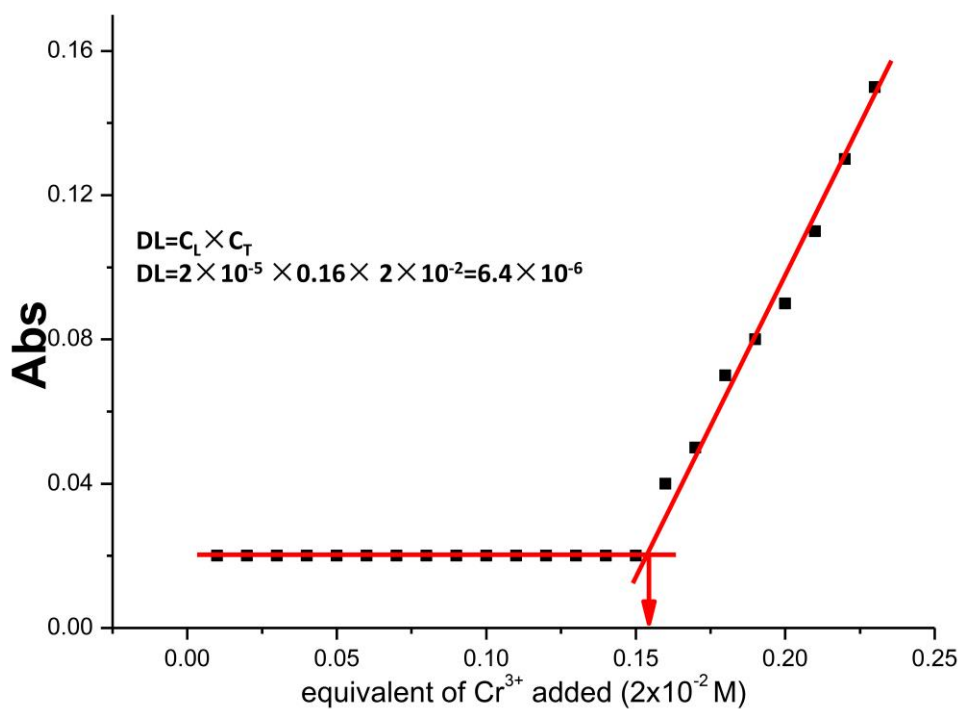
4. **Figure S4** UV-Vis spectra of **DYN3** (2×10^{-5} M) in $\text{CH}_3\text{CN}:\text{H}_2\text{O}$ (1:1, v/v, containing 0.01 M HEPES, pH=7.21) upon titration with 3.0 equiv. of perchlorate salts of metals. The red bars represent the absorbance of **DYN3** in the presence of 3 equiv. of cations of interest, respectively. The green bars represent the absorbance that occur upon the subsequent addition of 3 equiv. of Cr^{3+} to the above mentioned solutions, respectively. The absorbance measurements were recorded at 526 nm.



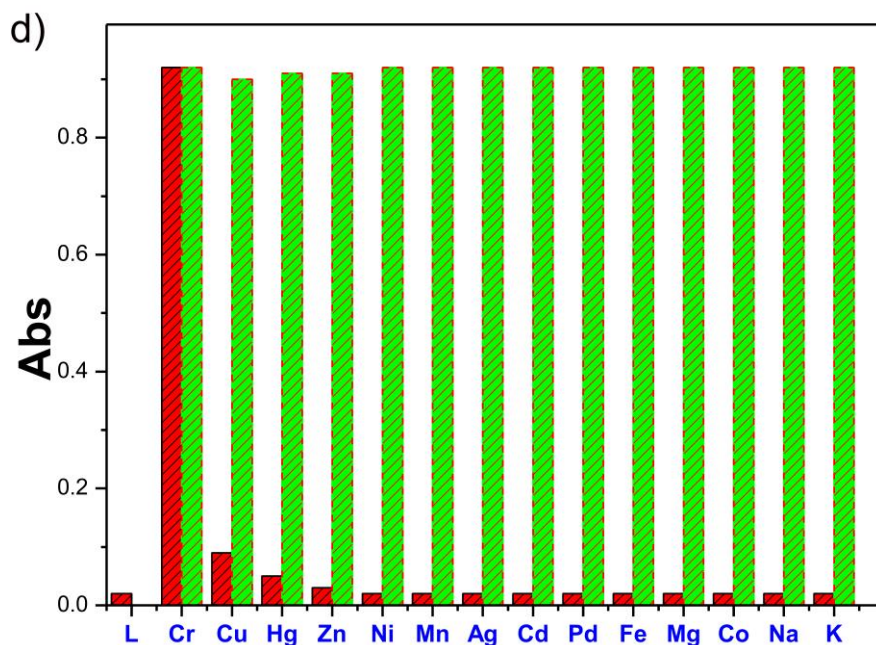
5. **Figure S5** The pH-dependent absorbance response of **DYN3** (20 μM) and **DYN3**+ Cr^{3+} in $\text{CH}_3\text{CN}/\text{H}_2\text{O}$ (1:1, v/v). The absorbance measurements were recorded at 526 nm.



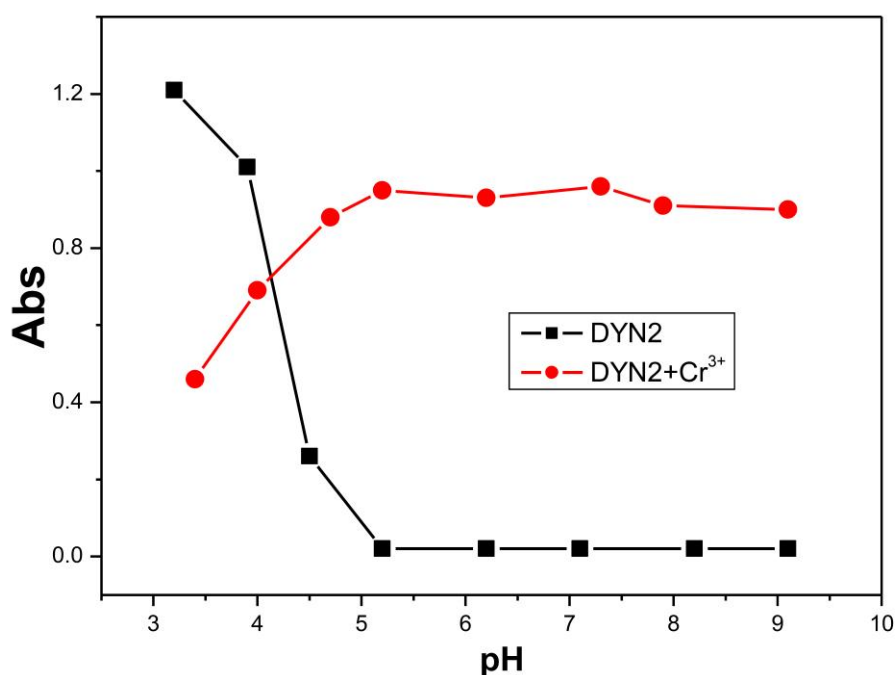
6. **Figure S6** Calculations for detection limit of **DYN3** with Cr^{3+} . The absorbance measurements were recorded at 526 nm.



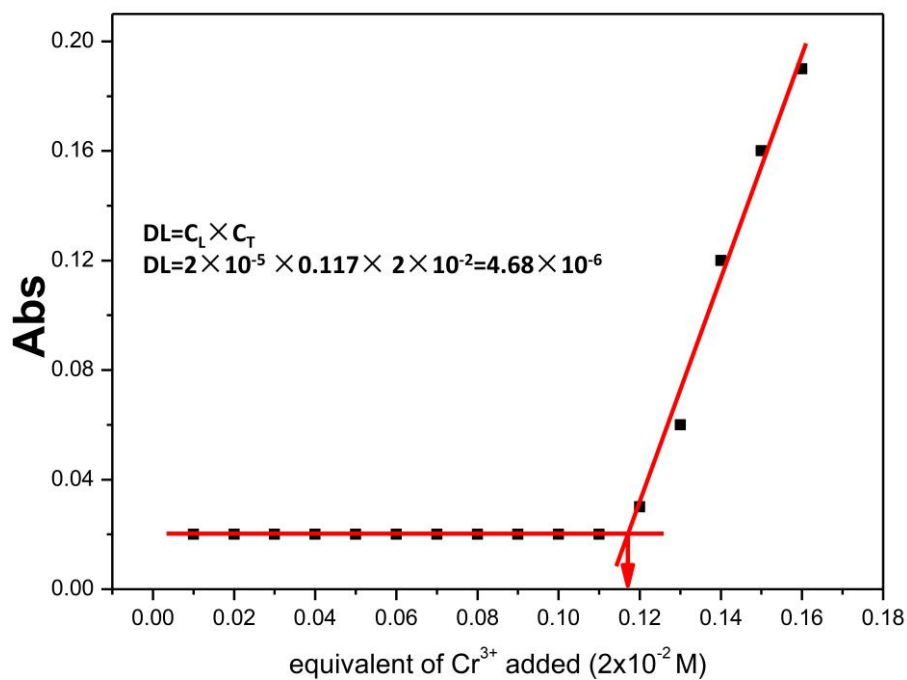
7. **Figure S7** UV-Vis spectra of **DYN2** (2×10^{-5} M) in $\text{CH}_3\text{CN}:\text{H}_2\text{O}$ (1:1, v/v, containing 0.01 M HEPES, pH=7.21) upon titration with 2.0 equiv. of perchlorate salts of metals. The red bars represent the absorbance of **DYN2** in the presence of 2 equiv. of cations of interest, respectively. The green bars represent the absorbance that occur upon the subsequent addition of 2 equiv. of Cr^{3+} to the above mentioned solutions, respectively. The absorbance measurements were recorded at 516 nm.



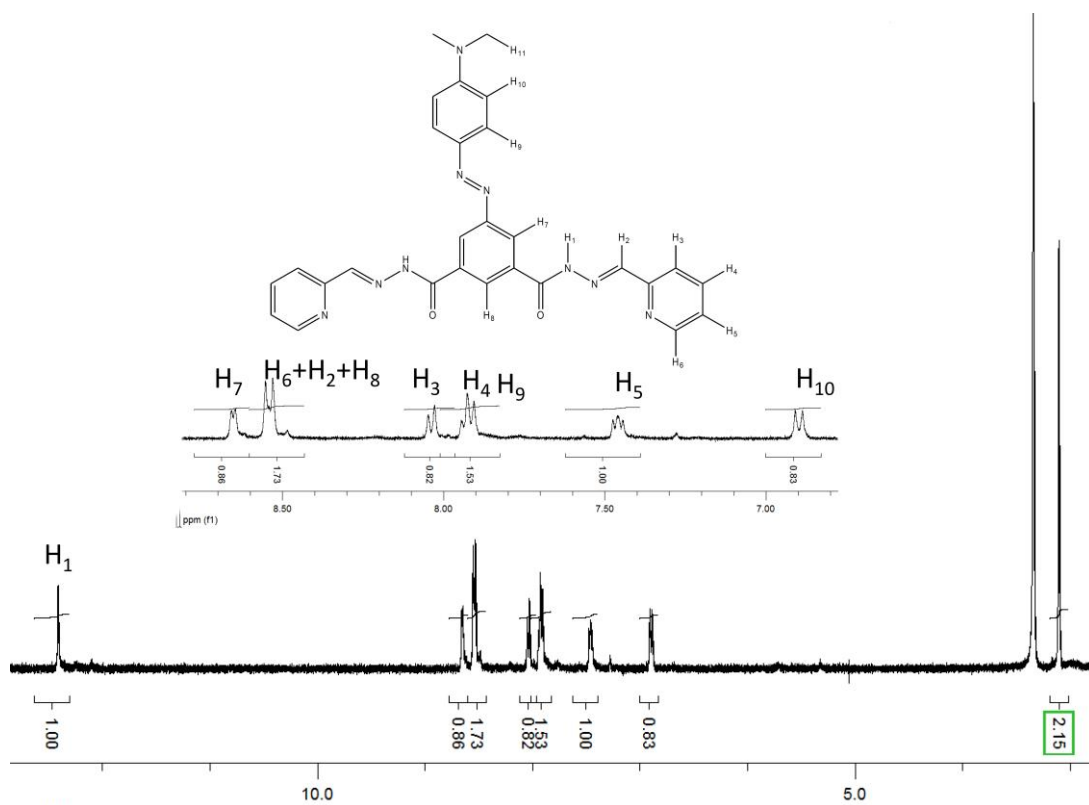
8. **Figure S8** The pH-dependent absorbance response of **DYN2** (20 μM) and **DYN2**+ Cr^{3+} in $\text{CH}_3\text{CN}/\text{H}_2\text{O}$ (1:1, v/v). The absorbance measurements were recorded at 516 nm.



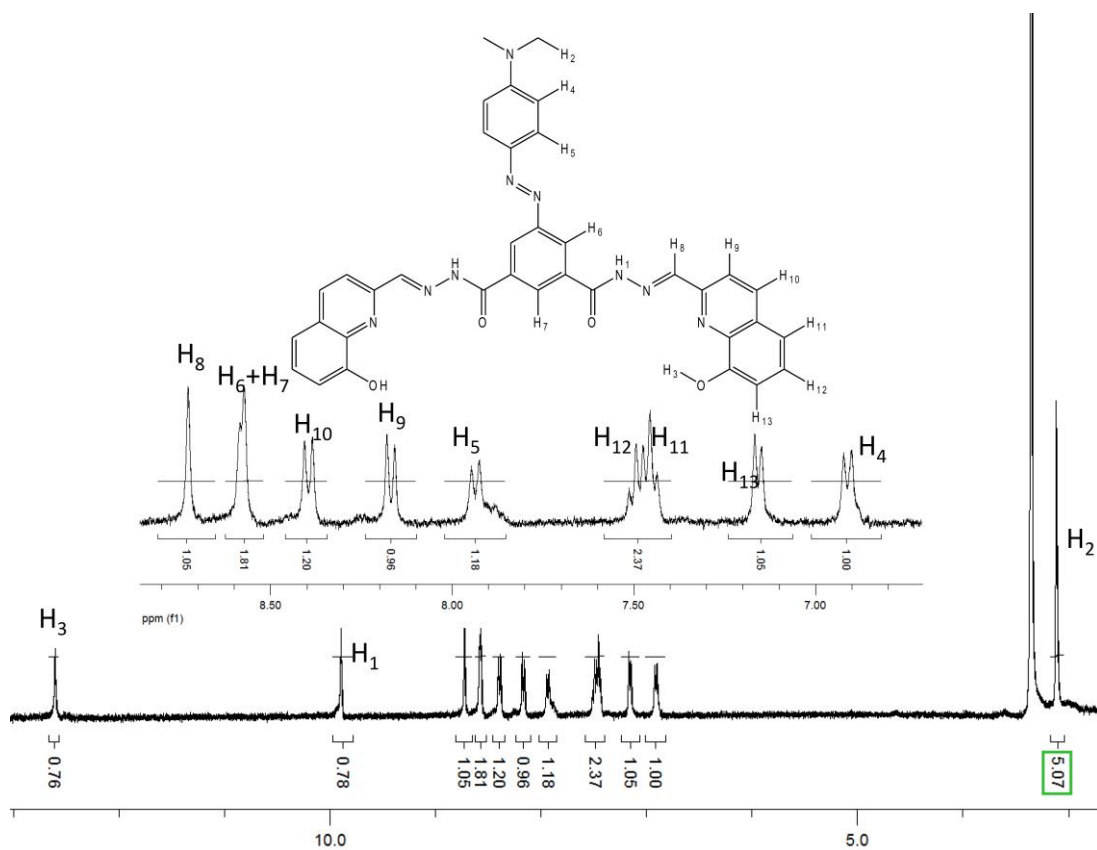
9. Figure S9 Calculations for detection limit of **DYN2** with Cr^{3+} . The absorbance measurements were recorded at 516 nm.



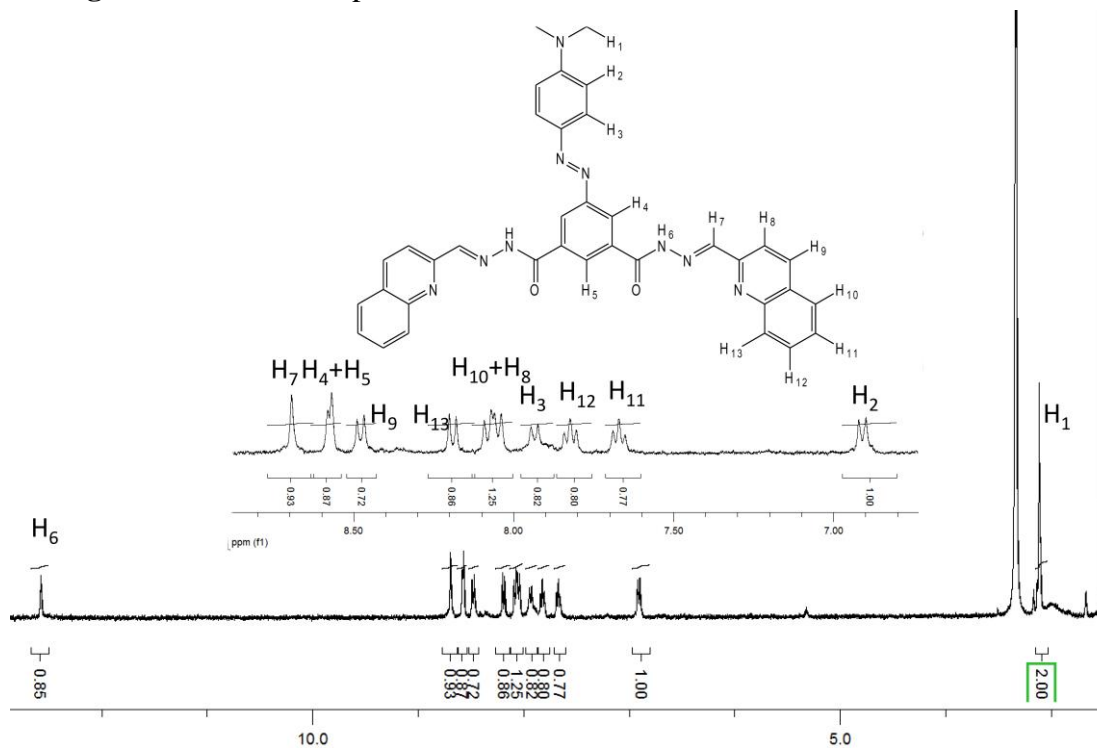
10. Figure S10 ^1H -NMR spectra of **DYN1**



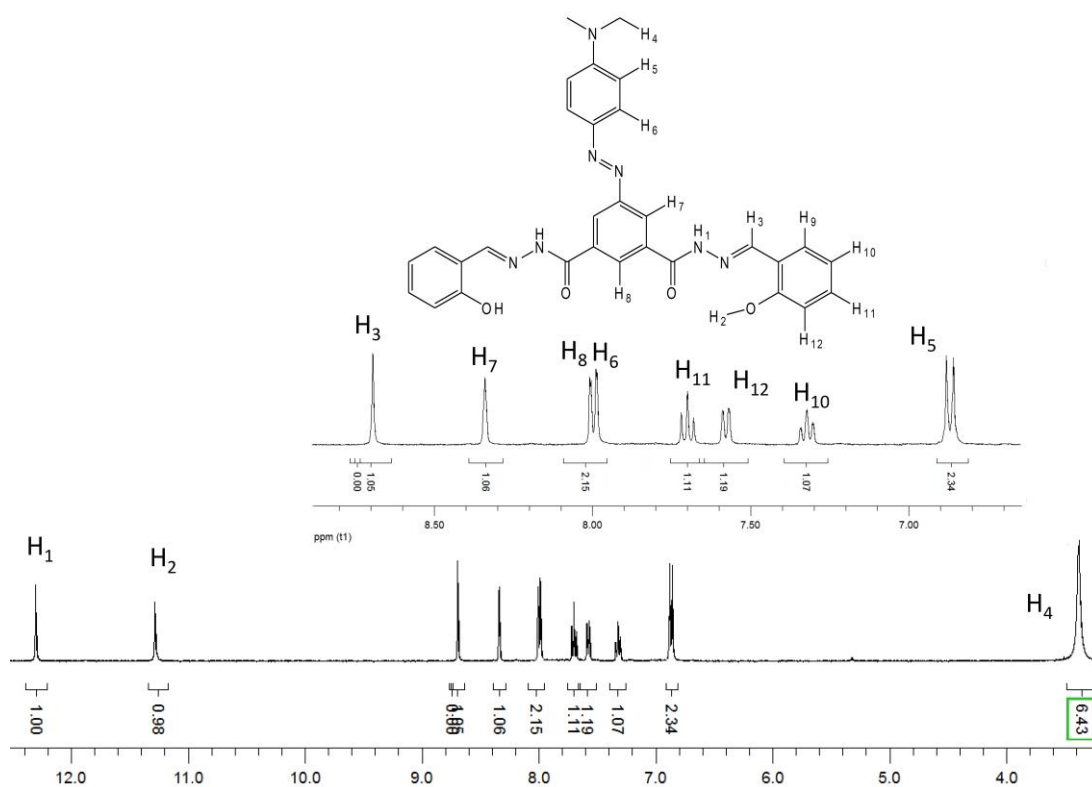
11. Figure S11 $^1\text{H-NMR}$ spectra of DYN3



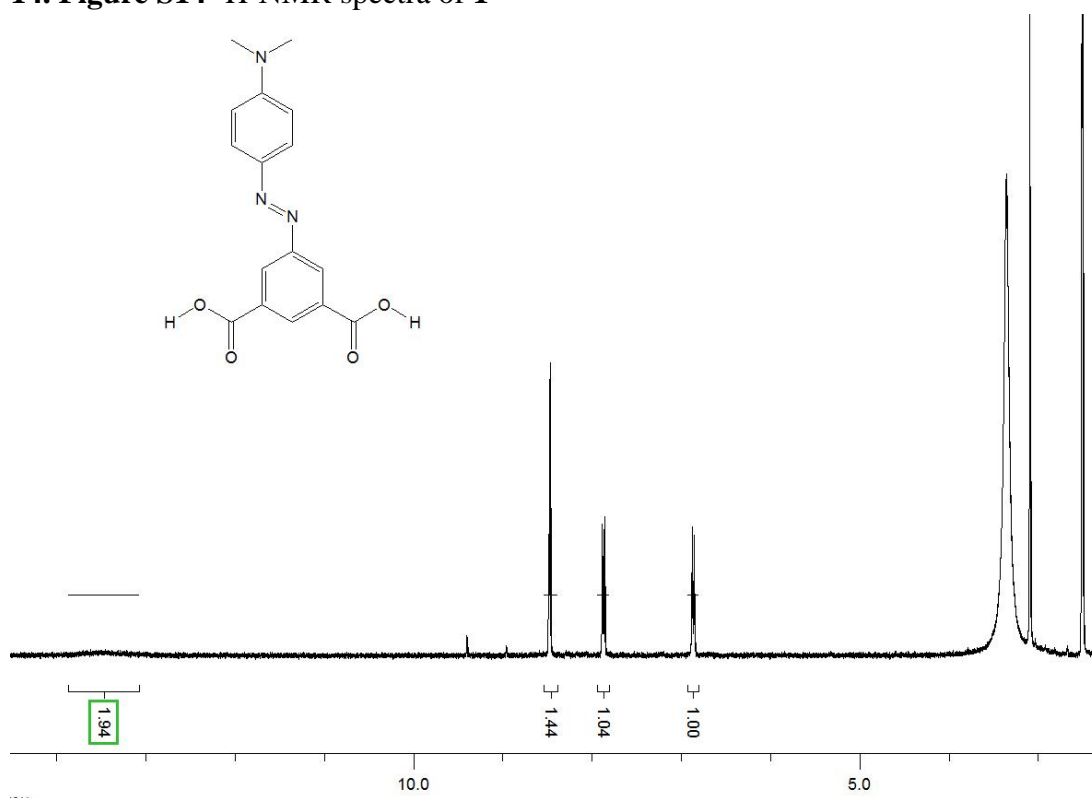
12. Figure S12 $^1\text{H-NMR}$ spectra of DYN2



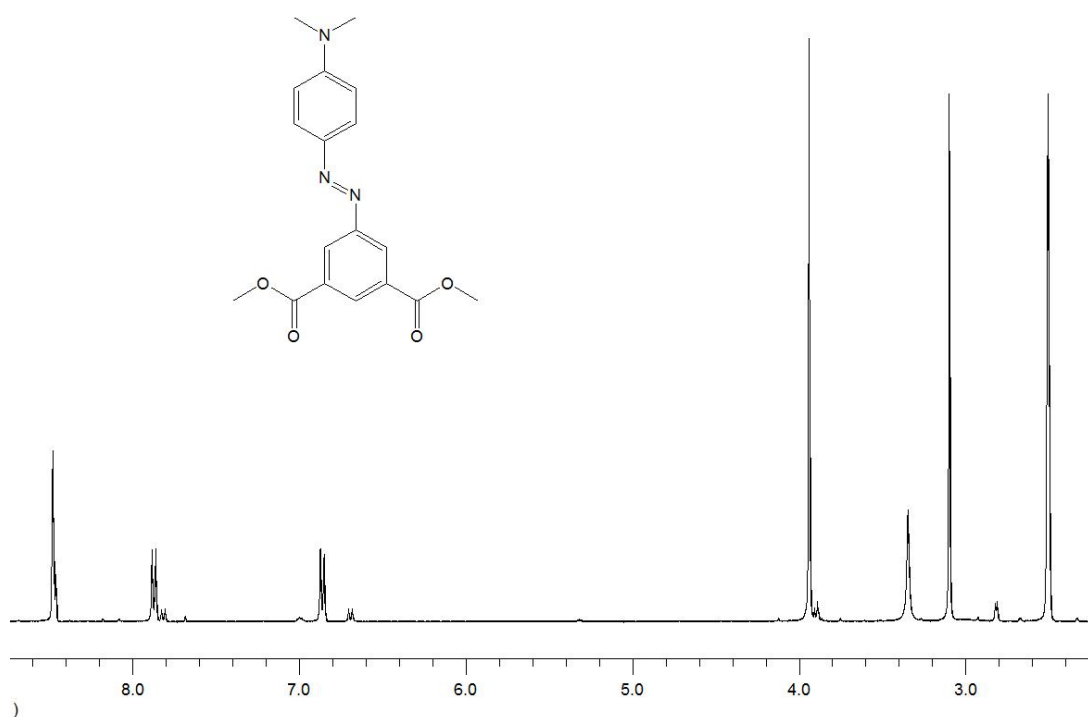
13. Figure S13 ¹H-NMR spectra of DYN4



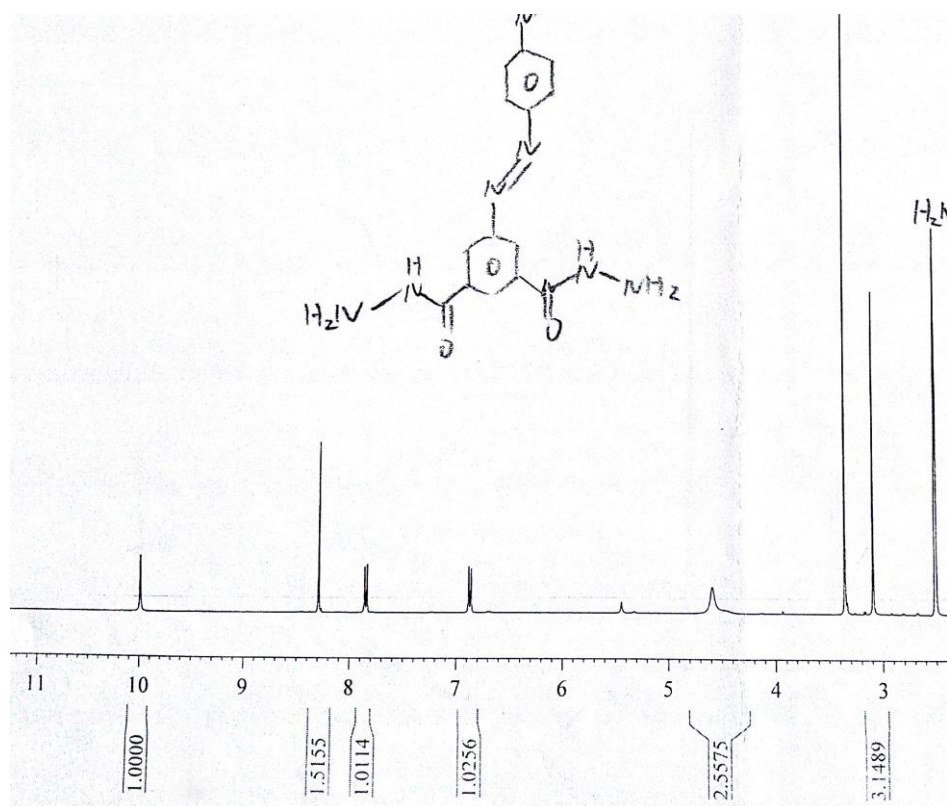
14. Figure S14 ¹H-NMR spectra of 1



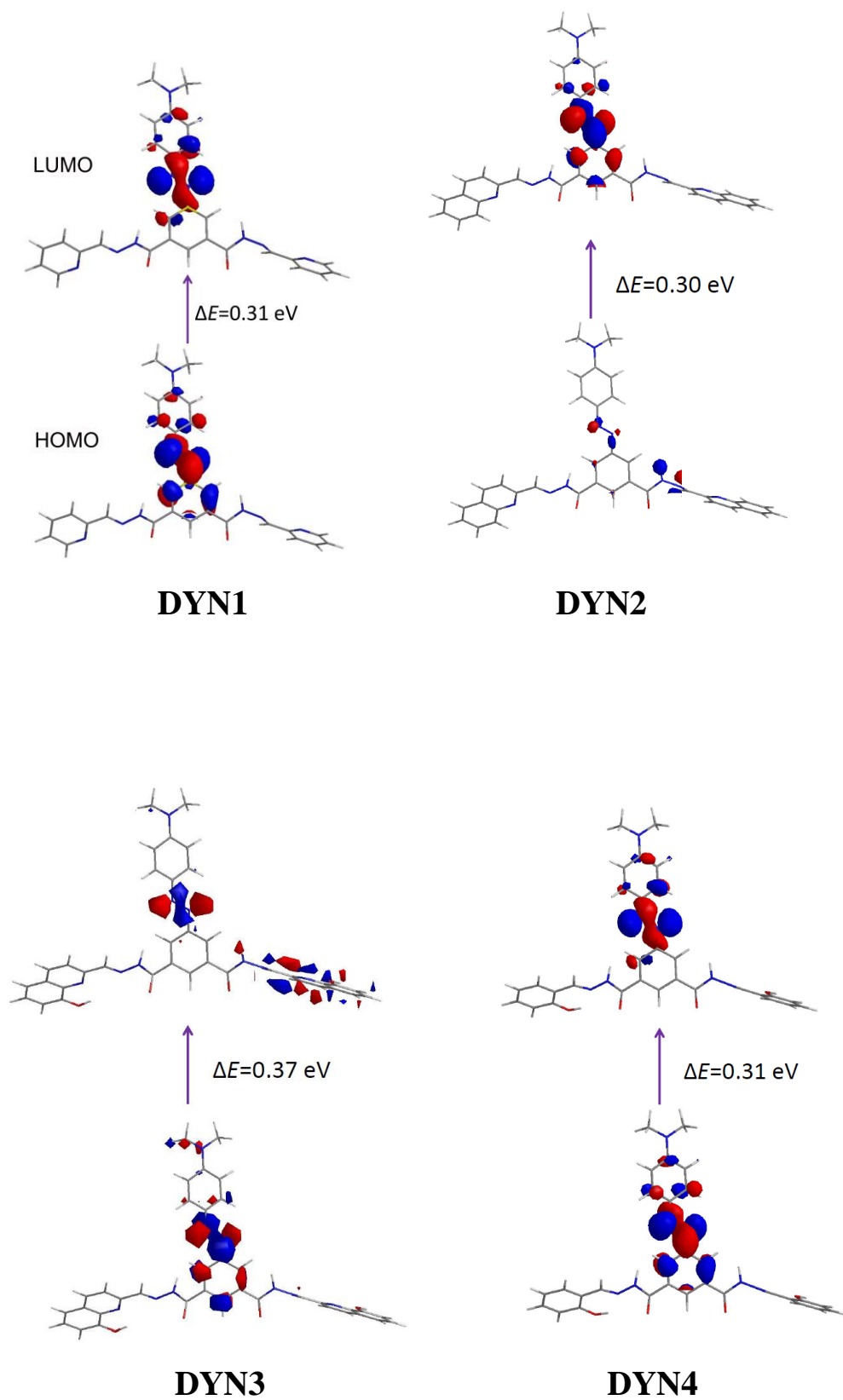
15. Figure S15 $^1\text{H-NMR}$ spectra of **2**



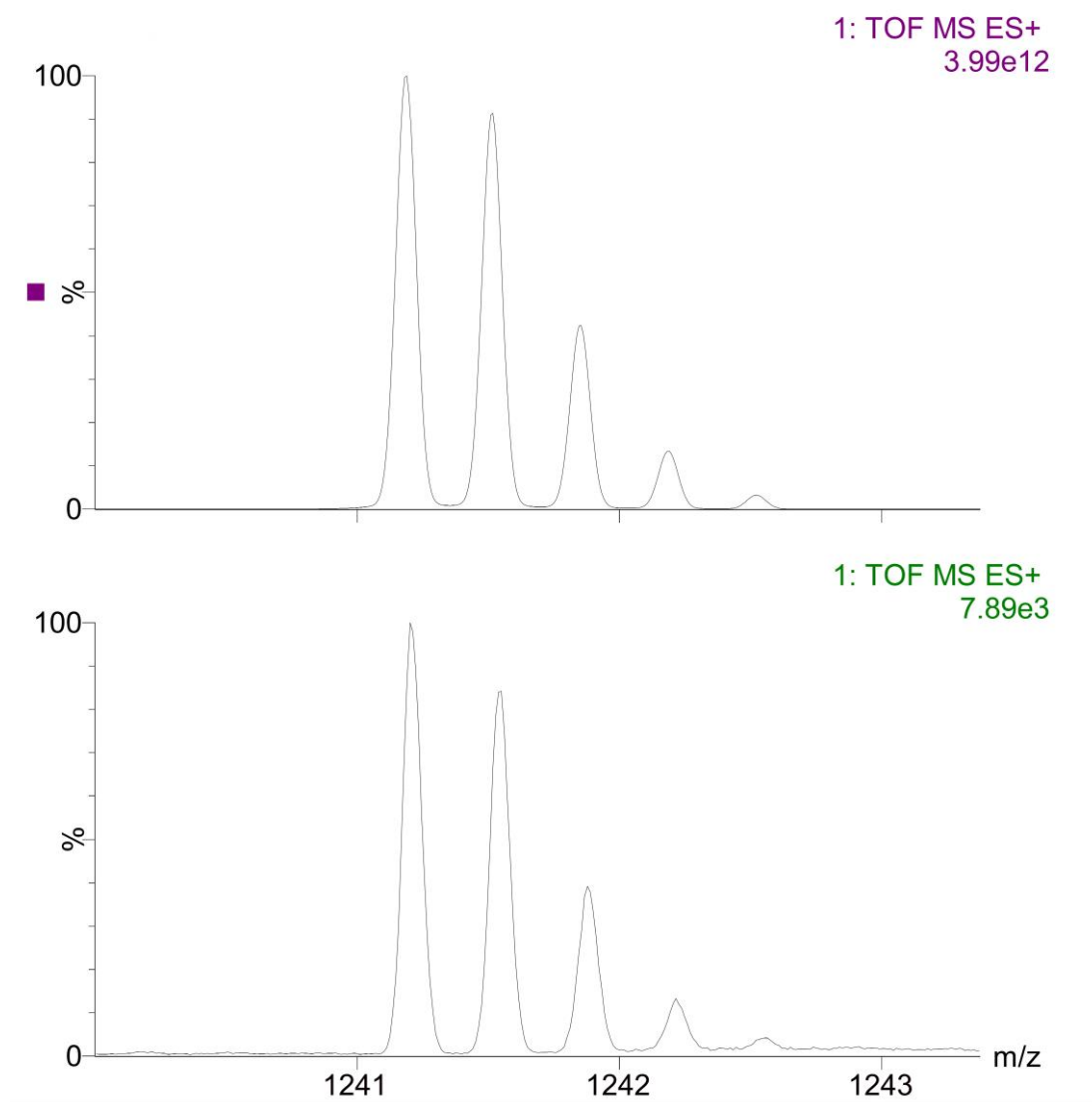
16. Figure S16 $^1\text{H-NMR}$ spectra of **3**



17. Figure S17 Contour plots of the HOMO and LUMO for DYN1-4

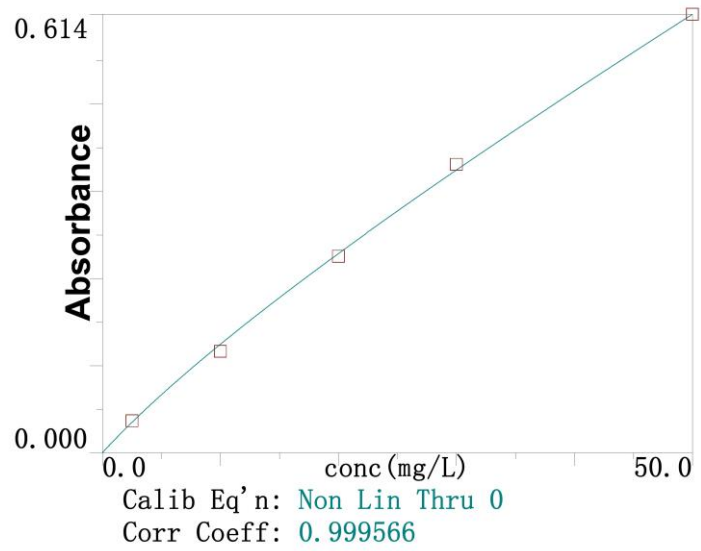


18. Figure S18 ESI-TOF spectra of **DYN1**+Cr³⁺. Comparison of the experimental peak (bottom) with the simulation results obtained on the basis of natural isotopic abundances (top).



19. Figure S19 ICP-AES spectra of sewage sample (bottom). Standard working curve (top).

Cr 357.87



Cr 357.87

Rep: 1

